CrossMark

ORIGINAL PAPER

Crustal deformation rates in Assam Valley, Shillong Plateau, Eastern Himalaya, and Indo-Burmese region from 11 years (2002–2013) of GPS measurements

Prakash Barman[1] · Sridevi Jade[1] · T. S. Shrungeshwara[1] · Ashok Kumar[2] ·
Sanjeev Bhattacharyya[2] · Jagat Dwipendra Ray[2] · Saigeetha Jagannathan[1] ·
Wangshi Menla Jamir[3]

Abstract The present study reports the contemporary deformation of the tectonically complex northeast India using 11 years (2002–2013) of GPS observations. The central Shillong Plateau and few sites north of Plateau located in Assam Valley behave like a rigid block with ~7 mm/year India-fixed southward velocity. The Euler pole of rotation of this central Shillong Plateau–Assam Valley (SH–AS) block is estimated to be at $-25.1° \pm 0.2°$N, $-97.8° \pm 1.8°$E with an angular velocity of $0.533° \pm 0.10°$ Myr^{-1} relative to India-fixed reference frame. Kopili fault located between Shillong Plateau and Mikir massif records a dextral slip of 4.7 ± 1.3 mm/year with a locking depth of 10.2 ± 1.4 km

indicating the fragmentation of Assam Valley across the fault. Presently, western edge of Mikir massif appears to be locked to Assam block indicating strain accumulation in this region. First-order elastic dislocation modelling of the GPS velocities estimates a slip rate of 16 mm/year along the Main Himalayan Thrust in Eastern Himalaya which is locked over a width of 130 km from the surface to a depth of 17 km with underthrusting Indian plate. Around ~9 mm/year arc-normal convergence is accommodated in Lesser Himalaya just south of Main Central Thrust indicating high strain accumulation. Out of 36 mm/year (SSE) India-Sunda plate motion, about ~16 mm/year motion is accommodated in Indo-Burmese Fold and Thrust Belt, both as normal convergence (~6 mm/year) and active slip (~7–11 mm/year) in this region.

✉ Sridevi Jade
sridevi@cmmacs.ernet.in

Prakash Barman
prakashb2002@gmail.com

T. S. Shrungeshwara
shrungeshsringeri@gmail.com

Ashok Kumar
ask@tezu.ernet.in

Sanjeev Bhattacharyya
bhattasanjeev@gmail.com

Jagat Dwipendra Ray
jagatgp@tezu.ernet.in

Saigeetha Jagannathan
saigeethaarun@gmail.com

Wangshi Menla Jamir
wangshijamir@yahoo.in

[1] CSIR-4PI, CSIR Fourth Paradigm Institute, (Formerly CSIR-CMMACS), Wind Tunnel Road, Bangalore 560 037, India

[2] Tezpur University, Tezpur, Assam 784028, India

[3] Nagaland University, Lumami, Nagaland 798 627, India

Introduction

The geodynamics of north-eastern segment of the Indian plate (Fig. 1) is of particular interest due to the simultaneous presence of the two plate boundary convergence zones namely the Himalayan arc and the Indo-Burmese Fold and Thrust Belt (IBFTB) and their confluence at the Assam syntaxis. The Shillong Plateau and its northern extension in Mikir hills are another distinct geological units of the region which adds to the tectonic complexity as well as seismicity (Table 1). The wedge-shaped Himalayan collision orogen is the result of India-Eurasian plate collision since ~50 Ma and absorbs ~20 mm/year India-Eurasia convergence along the Main Himalayan Thrust (MHT)
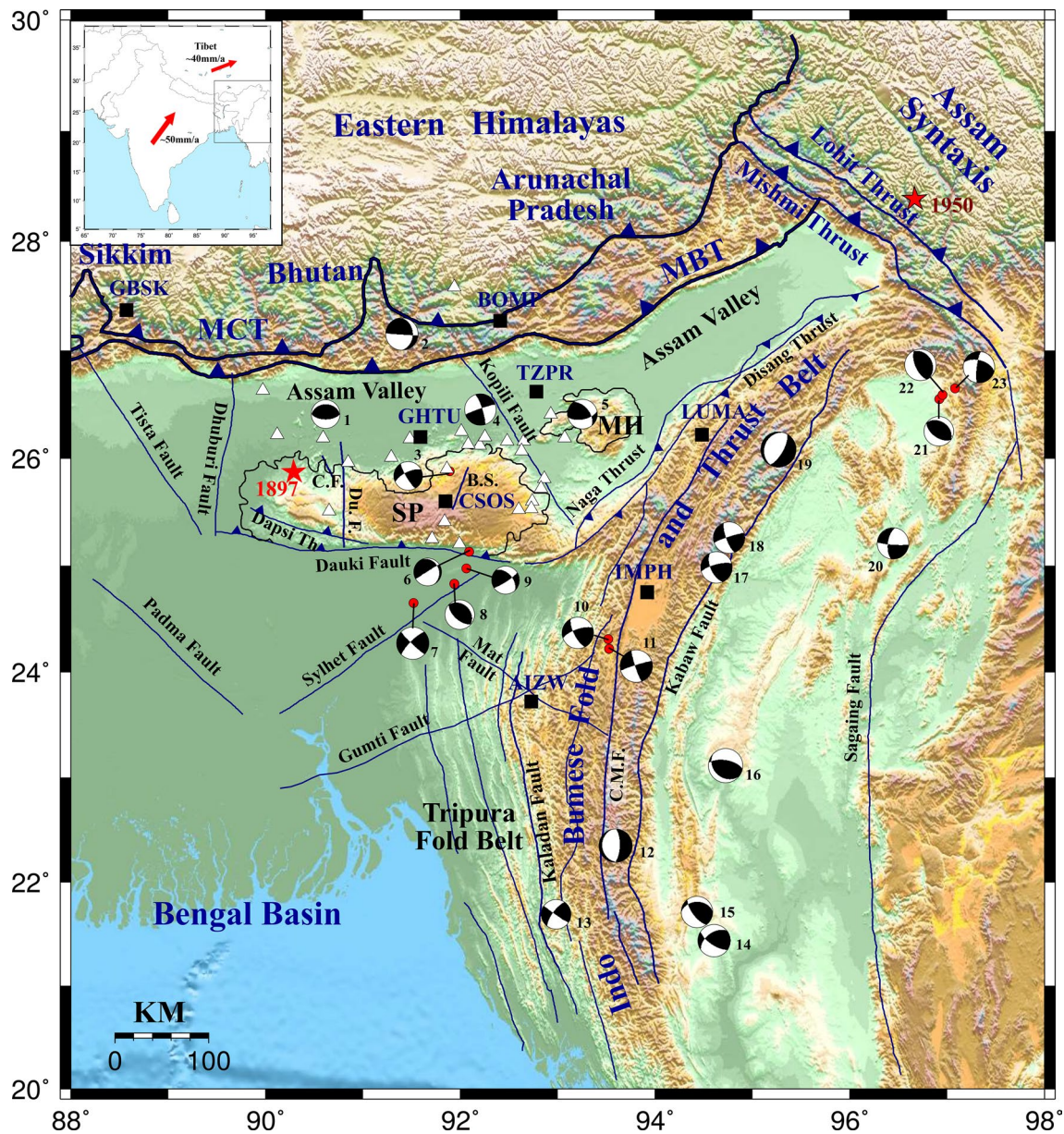
Fig. 1 Tectonic setting of the north-eastern Indian Plate. The *fault lines* (Bhattacharya et al. 2008; Kayal et al. 2012; Gahalaut et al. 2013) and the earthquake focal mechanisms (Ni et al. 1989; Chen and Molnar 1990; Kayal et al. 2012) are from published literatures. *Numbers* next to focal mechanism identifies the earthquake, and the details of the events are given in Table 1. *Black rectangles* represent permanent GPS stations and *white triangles* represent campaign mode GPS station. The Sunda plate is situated to the east from 100° to 120°E. *MCT* Main Central Thrust, *MBT* Main Boundary Thrust, *C.F.* Chedrang Fault, *Du. F.* Dudhnoi fault, *B.S.* Barapani Shear Zone, *C.M.F.* Churachandpur-Mao Fault, *SP* Shillong Plateau, *MH* Mikir Hills

(Bilham et al. 1997). Along the MHT, the Indian plate underthrust beneath the Eurasian plate resulting in crustal shortening, rising Himalaya and high seismicity. The Main Central Thrust (MCT) and Main Boundary Thrust (MBT) from north to south are the prominent thrusts listric to the MHT. The Main Frontal Thrust (MFT) is considered as the surface expression of the MHT that marks the end of the Himalayan orogen towards south. The India-Sunda convergence zone towards the east of northeast India is the result

of India-Eurasia plate collision where the Indian plate is subducting beneath the Burmese microplate (Ni et al. 1989; Guzmán-Speziale and Ni 1996; Gahalaut et al. 2013). The India-Sunda convergence zone is broadly divided into Sagaing fault to the east and Indo-Burmese Fold and Thrust Belt (IBFTB) to the west. Out of ~36 mm/year India-Sunda relative plate motion (Socquet et al. 2006), ~20 ± 3 mm/year is accommodated in the Sagaing fault through right-lateral strike-slip motion and the remaining ~18 ± 2 mm/

Table 1 Source parameters of past earthquakes of northeast India (plotted in Fig. 1) from the published literatures (Ni et al. 1989; Chen and Molnar 1990; Kayal et al. 2012)

Event no.	Date	Lon (°E)	Lat (°N)	Depth (km)	Strike (°)	Dip (°)	Rake (°)	Magnitude
1	18/08/1968	90.62	26.42	29	90	60	90	5.1
2	21/09/2009	91.47	27.24	14	1	32	177	6.3
3	05/10/1999	91.89	25.88	33	244	68	12	5.2
4	19/08/2009	92.30	26.49	10	342	80	−175	5.1
5	17/07/1971	93.15	26.41	36	79	60	46	5.4
6	21/06/1963	92.09	25.13	38	238	88	−70	5
7	06/02/1988	91.52	24.65	32	225	77	5	5.8
8	12/06/1968	91.94	24.83	41	132	60	90	5.3
9	19/06/1963	92.06	24.97	52	57	80	42	5
10	06/05/1984	93.53	24.22	60	153	70	159	5.7
11	31/05/1973	93.52	24.31	48	162	84	175	5.8
12	22/01/1964	93.58	22.33	55	2	69	−85	6.0
13	12/05/1977	92.96	21.68	40	216	72	3	5.4
14	08/07/1975	94.62	21.42	120	124	68	136	5.9
15	27/02/1964	94.40	21.65	90	143	68	118	5.7
16	17/10/1969	94.70	23.09	132	280	63	75	6.1
17	29/12/1971	94.72	25.17	65	160	75	174	5.6
18	30/08/1983	94.67	25.04	62	255	74	31	5.7
19	29/07/1970	95.37	26.02	75	196	22	−103	6.4
20	30/05/1971	96.40	25.20	10	187	63	−173	5.6
21	30/05/1975	96.92	26.55	12	156	63	93	5.7
22	03/06/1975	96.95	26.59	10	126	55	92	5.4
23	28/11/1984	97.08	26.65	6	285	54	13	5.7

year is accommodated in IBFTB (Vigny 2003; Socquet et al. 2006; Maurin et al. 2010; Gahalaut et al. 2013). The Assam syntaxis is a complex geodynamic area where crustal material flow is clockwise and modelled by Copley and McKenzie (2007) as visco-elastic crustal or lithospheric flow. Assam Syntaxis consists a series of parallel thrusts like the Lohit, Tidding, Mishimi and was the site for the great Assam Earthquake of 1950 ($M_w = 8.5$) (Ben-Menahem et al. 1974; Chen and Molnar 1977).

Apart from these plate convergence orogens, the Shillong Plateau (Fig. 1) and its eastern extension in Mikir Hills situated at the mid Assam Valley are the sources of intra-plate seismicity of the region. The great 1897 intra-plate earthquake ($M_w = 8.1$) occurred towards the north-western limit of the Shillong Plateau (Oldham 1899). The near perfect curvature of Himalayan arc that can be seen in its western and central sections breaks near longitude of the western margin (90°E) of the Shillong Plateau (Clark and Bilham 2008). The upheaval of Shillong Plateau in the past 2–5 Ma is believed to lower the seismicity of the Bhutan Himalaya (Bilham and England 2001) but at the same time, raises the seismic risk of neighbouring Bangladesh (Jade et al. 2007). The Shillong Plateau is separated from Mikir massif by the NW–SE trending Kopili fault which is reported to be seismically highly active (Bhattacharya et al. 2008; Kayal et al. 2012). The Bengal basin (also known

as Surma basin), which act like reservoir for the Himalayan sediments transported by the Ganga, Brahmaputra, and Meghna Rivers, lies south of the Shillong Plateau. The E–W trending Dauki fault marks the southern margin of the Shillong Plateau and separates the Shillong Plateau from the Bengal basin. Within the Shillong Plateau, NW–SE trending Dapsi fault which is the north-western extension of Dauki fault separates the Cretaceous–Tertiary sediments to the south and Precambrian Gneissic complex to the north. Chedrang fault and Dudhnoi fault lying towards the north-west of the plateau were activated during the 1897 great Shillong earthquake (Kayal and De 1991).

For the first time, GPS-based crustal deformation studies were initiated in the northeast India in the year 1997. Using GPS measurements spanning 1997–1999, south-ward velocity of 6.3 ± 3.8 mm/year of central Shillong relative to India-fixed reference frame was reported (Paul et al. 2001). This result was the first to show that northeast India exhibits different tectonic movement compared to the Indian shield. Insignificant deformation was reported within the Shillong Plateau using GPS measurements spanning 1997–2006 (Jade et al. 2007). Across eastern Himalaya, ~16 mm/year arc-normal convergence is reported by Jade et al. (2007), which is distributed between higher and lesser Himalaya. Variable convergence rates across Shillong Plateau and IBFTB and possible

existence of an active transverse zone between Tripura-Mizoram Salient and Imphal recess (Fig. 5) were reported on the basis of converging baselines (Jade et al. 2007). In addition, ~8–9 mm/year of E–W convergence is reported between IBFTB and eastern-central parts of the Shillong Plateau (Mukul et al. 2010). Another study using GPS data from 2003 to 2011 reported 6 ± 1.5 mm/year convergence of Shillong Plateau relative to the Indian plate (Mahesh et al. 2012). They also reported 3 ± 1.5 mm/year dextral motion in the Kopili fault. Oblique convergence of ~20 mm/year between Indian and Eurasian plate in frontal Eastern Himalayan Syntaxis is reported using GPS measurements (Devachandra et al. 2014). Recently based on GPS data, it has been reported that the Assam Valley (also known as Brahmaputra Valley) rotates clockwise relative to India (Vernant et al. 2014). They reported further that the Assam Valley is divided into two distinct regions separated by Kopili fault. In this paper, we update the present-day active deformation pattern pertaining to the prominent tectonic domains of the northeast India for the first time using long-period GPS measurements from 2002 to 2013 collected from 26 campaign mode (Fig. 1; Table 2) and eight continuously operated GPS sites. We extend the span of continuous GPS measurements in northeast India from earlier reported 3–4 years (Jade et al. 2007) to 7–10 years thereby reducing the horizontal uncertainties by 35 %. In addition, we present velocities for 24 new campaign mode sites in this region.

Data and methods

The GPS data set used for the study comprises measurements from 26 survey-mode GPS sites (Fig. 1; Table 2) and eight continuously operated GPS sites, spread across different tectonic domains of the north-eastern India spanning the period 2002–2013. The study presents data from 24 new campaign sites and additional data of 7 years (2006–2013) from the eight continuously operated GPS sites that were presented in Jade et al. (2007). Two campaign sites TAWA and MUNN are earlier sites with three additional epochs of new data. The campaign sites are located on bedrock exposures with drilled 2–3 mm diameter hole marks for subsequent reoccupations. Twenty campaign sites have 5–7 epochs of data, six sites have 3–4 epochs, and each epoch is separated by more than a year with 3–6 days of data per year. The GPS antennas of the permanent sites are secured on concrete pillars grouted to bedrock. Continuous data are available 365 days (24 × 7) a year except for few data gaps when the sites had operational issues. Continuous GPS data from nine IGS sites namely BAN2, IISC, HYDE, KIT3, KUNM, LHAZ, POL2, SELE, and WUHN were included in the processing to tie our regional sites

to the International Terrestrial Reference Frame (ITRF) (Altamimi et al. 2011)

All the GPS data are thoroughly quality checked using TEQC (Translation, editing, and quality check) toolkit by UNAVCO (Estey and Meertens 1999) for high multi-path and cycle-slips. In the analysis, data with high multi-path, high cycle-slips, and observations less than 12 h were omitted. The phase processing of the GPS data was accomplished using GAMIT/GLOBK (Herring et al. 2010a, b) version 10.4 following the methodology described by Dong et al. (1998). The signal carrier phase ambiguities are resolved by forming wide lane and the best-integer-estimation using the ambiguity free estimates for the narrow lane combination of phase and pseudo-ranges. The first-order ionospheric delays are eliminated by forming LC linear combination. To eliminate second and third order ionospheric refraction terms from the carrier signal (Petrie et al. 2010), we have used daily IONEX files containing global ionospheric maps of vertical Total Electron Content distributed by CODE (Schaer et al. 1998). The signal delay caused by the troposphere at each station was estimated by incorporating a piecewise-linear model with stochastic constraints. The loosely constrained network solutions from GAMIT were combined to define the reference frame by minimizing the misfit of the IGS reference sites' coordinates and velocities to their ITRF08 (Altamimi et al. 2011) values by performing the six parameter Helmert transformation. The long-period noise that affects the velocity estimates of sites was accounted by adding random walk noise for each velocity components determined using the first-order Gauss–Markov extrapolation (FOGMEX) algorithm (Herring 2003; Reilinger et al. 2006). For the survey-mode GPS sites, median random walk noise 4.04×10^{-7}, 3.39×10^{-7} m²/year (6.3, 5.8 mm/year$^{1/2}$ in N, E) generated for the permanent GPS sites by the FOGMEX algorithm was added. The ITRF08 velocities were transformed to India-fixed reference frame by using the most recent estimate of Euler pole of rotation (Mahesh et al. 2012) of the stable Indian plate located at 51.41° ± 0.07°N, 8.97° ± 0.8°E with an angular velocity of 0.539° ± 0.002°/Myr.

Dislocation modelling

The dislocation modelling is based on the Okada dislocation theory (Okada 1985) and weighted least-square inversion. The observation equation for surface displacement d for a finite rectangular fault in an elastic half space is given by:

$$d = Gm \tag{1}$$

where G denotes the Green's functions which is a function of fault parameters (length, width, depth, dip, and strike)

Table 2 Earthquake parameters site velocities estimated in ITRF08 and India-fixed reference frame

SITE CODE site name	Lat (°N)	Lon (°E)	ITRF08 (mm/year)		India-fixed (mm/year)		Rho	GPS data	Tectonic domain
			Ve	Vn	Ve	Vn			
AMSO Amsoi	26.16	92.48	39.76 ± 1.00	26.96 ± 0.95	−0.54 ± 1.00	−10.22 ± 0.95	−0.045	5 Epochs (2007–2012)	Assam Valley
BURA Bura Mayong	26.25	92.01	39.14 ± 0.65	28.72 ± 0.62	−0.99 ± 0.65	−8.42 ± 0.62	−0.045	5 Epochs (2007–2012)	Assam Valley
GHTU* Gauhati University	26.15	91.66	39.66 ± 0.15	29.91 ± 0.17	−0.41 ± 0.15	−7.21 ± 0.17	0.053	2003–2011	Assam Valley
JAGI Jagiroad	26.12	92.2	39.38 ± 0.67	27.77 ± 0.63	−0.86 ± 0.67	−9.39 ± 0.63	0.02	5 Epochs (2007–2012)	Assam Valley
KHET Khetri	26.13	92.08	39.13 ± 0.62	28.57 ± 0.58	−1.07 ± 0.62	−8.58 ± 0.58	0.004	5 Epochs (2007–2012)	Assam Valley
KUMO Kumoi	26.2	92.25	38.51 ± 0.54	26.36 ± 0.50	−1.71 ± 0.54	−10.80 ± 0.50	0.016	5 Epochs (2007–2012)	Assam Valley
MAHA Mahamaya	26.22	90.12	39.35 ± 0.37	33.27 ± 0.34	−0.25 ± 0.37	−3.70 ± 0.34	0.009	5 Epochs (2004–2013)	Assam Valley
PANC Pancharatna	26.19	90.59	39.00 ± 0.28	30.75 ± 0.28	−0.75 ± 0.28	−6.27 ± 0.28	0.044	6 Epochs (2004–2013)	Assam Valley
RAIM Raimana	26.63	89.97	39.95 ± 0.30	33.67 ± 0.29	0.58 ± 0.30	−3.29 ± 0.29	0.014	5 Epochs (2004–2013)	Assam Valley
TZPR* Tezpur	26.62	92.78	40.60 ± 0.18	26.97 ± 0.14	0.41 ± 0.18	−10.23 ± 0.14	0.068	2003–2013	Assam Valley
BOMP* Bomdila	27.27	92.41	41.88 ± 0.16	19.87 ± 0.55	2.08 ± 0.16	−17.30 ± 0.55	0.017	2004–2013	Eastern Himalaya
TAWA Tawang	27.58	91.94	46.80 ± 0.27	13.91 ± 0.26	7.28 ± 0.27	−23.23 ± 0.26	−0.039	5 Epochs (2002–2013)	Eastern Himalaya
AIZW* Aizwal	23.72	92.73	35.01 ± 1.02	28.36 ± 0.66	−6.36 ± 1.02	−8.84 ± 0.66	−0.003	2004–2006	Indo-Burmese Fold and Thrust Belt
IMPH* Imphal	24.75	93.92	29.75 ± 0.37	19.38 ± 0.32	−11.53 ± 0.37	−17.90 ± 0.32	0.01	2004–2006	Indo-Burmese Fold and Thrust Belt
LUMA* Lumami	26.22	94.48	37.97 ± 0.17	21.84 ± 0.47	−2.87 ± 0.17	−15.46 ± 0.47	0.025	2004–2013	Indo-Burmese Fold and Thrust Belt
KAMP Kampur	26.16	92.65	39.69 ± 0.95	28.55 ± 0.84	−0.66 ± 0.95	−8.64 ± 0.84	0.024	5 Epochs (2007–2012)	Kopili Gap
KHER Kheroni	25.81	92.86	40.37 ± 0.46	27.66 ± 0.44	−0.18 ± 0.46	−9.55 ± 0.44	0.004	4 Epochs (2007–2012)	Kopili Gap
PANI Panimura	25.72	92.83	38.07 ± 0.46	29.19 ± 0.46	−2.51 ± 0.46	−8.02 ± 0.46	−0.001	4 Epochs (2006–2012)	Kopili Gap
RAJA Raja Ali	26.07	92.63	38.76 ± 0.49	28.89 ± 0.49	−1.62 ± 0.49	−8.30 ± 0.49	0.038	5 Epochs (2007–2012)	Kopili Gap
SOKR Sokra Pam	25.6	92.74	38.94 ± 0.91	27.51 ± 0.90	−1.67 ± 0.91	−9.69 ± 0.90	0.062	3 Epochs (2006–2011)	Kopili Gap
UMRA Umrangsho	25.53	92.73	38.24 ± 0.54	27.10 ± 0.52	−2.40 ± 0.54	−10.10 ± 0.52	0.021	3 Epochs (2006–2011)	Kopili Gap
BORJ Borjuri	26.41	92.93	39.71 ± 0.28	26.30 ± 0.28	−0.61 ± 0.28	−10.91 ± 0.28	0.022	5 Epochs (2004–2013)	Mikir Hills
DOKM Dokmoka	26.19	93.07	39.37 ± 0.79	26.22 ± 0.75	−1.08 ± 0.79	−11.00 ± 0.75	0.047	6 Epochs (2004–2013)	Mikir Hills
BAMU Bamunigaon	26.01	91.29	40.11 ± 0.32	30.33 ± 0.31	0.08 ± 0.32	−6.75 ± 0.31	0.034	6 Epochs (2004–2013)	Shillong Plateau
CSOS* Shillong	25.57	91.86	39.56 ± 0.22	29.71 ± 0.20	−0.82 ± 0.22	−7.42 ± 0.20	0.043	2003–2008	Shillong Plateau
GARO Garogaon	25.96	90.85	39.88 ± 0.34	30.55 ± 0.32	−0.04 ± 0.34	−6.49 ± 0.32	0.093	4 Epochs (2005–2013)	Shillong Plateau
MAWR Mawriang	25.2	91.99	39.73 ± 0.37	29.82 ± 0.34	−0.84 ± 0.37	−7.32 ± 0.34	−0.026	6 Epochs (2004–2013)	Shillong Plateau
MUNN Munn	25.41	91.84	38.73 ± 0.25	29.59 ± 0.24	−1.71 ± 0.25	−7.54 ± 0.24	0.032	7 Epochs (2002–2013)	Shillong Plateau
NATU Natun Bazar	25.52	92.6	40.06 ± 0.81	28.89 ± 0.81	−0.54 ± 0.81	−8.30 ± 0.81	−0.068	5 Epochs (2006–2011)	Shillong Plateau
NONG Nongpoh	25.9	91.86	39.33 ± 0.28	29.86 ± 0.29	−0.91 ± 0.28	−7.27 ± 0.29	0.029	6 Epochs (2004–2013)	Shillong Plateau
RANG Rangsangbo	25.25	91.71	39.67 ± 0.60	32.44 ± 0.57	−0.80 ± 0.60	−4.68 ± 0.57	0.028	7 Epochs (2003–2013)	Shillong Plateau

Table 2 continued

SITE CODE site name	Lat (°N)	Lon (°E)	ITRF08 (mm/year)		India-fixed (mm/year)		Rho	GPS data	Tectonic domain
			Ve	Vn	Ve	Vn			
WLMN William Nagar	25.51	90.65	40.54 ± 0.35	32.67 ± 0.32	0.48 ± 0.35	−4.36 ± 0.32	−0.025	4 Epochs (2005–2012)	Shillong Plateau
GBSK* Panthang	27.37	88.57	39.49 ± 0.31	28.65 ± 0.32	0.87 ± 0.31	−8.15 ± 0.32	0.007	2004–2008	Sikkim Himalaya
BAN2# Bangalore	13.03	77.51	41.93 ± 0.20	35.67 ± 0.14	−0.74 ± 0.20	0.83 ± 0.14	0.084	2002–2013	Southern Indian Plate
HYDE# Hyderabad	17.42	78.55	40.36 ± 0.31	34.99 ± 0.17	−0.55 ± 0.31	−0.09 ± 0.17	0.058	2002–2013	Southern Indian Plate
IISC# Bangalore	13.02	77.57	41.94 ± 0.20	35.66 ± 0.14	−0.74 ± 0.20	0.81 ± 0.14	0.084	2002–2013	Southern Indian Plate
KIT3# Kitab	39.13	66.89	28.09 ± 0.18	5.38 ± 0.19	4.12 ± 0.18	−26.30 ± 0.19	−0.054	2002–2013	Eurasian Plate
KUNM# Kunming	25.03	102.8	31.38 ± 0.22	−18.90 ± 0.17	−12.22 ± 0.22	−56.24 ± 0.17	0.026	2002–2013	Eurasian Plate
LHAZ# Lhasa	29.66	91.1	46.13 ± 0.14	15.13 ± 0.16	7.83 ± 0.14	−21.93 ± 0.16	0.049	2002–2013	Eurasian Plate
POL2# Kyrgyzstan	42.68	74.69	27.51 ± 0.10	4.75 ± 0.10	3.34 ± 0.10	−29.33 ± 0.10	−0.043	2002–2013	Eurasian Plate
SELE# Kazakhstan	43.18	77.02	28.26 ± 0.12	3.84 ± 0.13	3.51 ± 0.12	−30.83 ± 0.13	−0.01	2002–2013	Eurasian Plate
WUHN# China	30.53	114.36	31.09 ± 0.19	−13.28 ± 0.18	−14.39 ± 0.19	−49.35 ± 0.18	0.083	2002–2013	Eurasian Plate

The sites marked with * are permanent GPS stations, and those marked with # are IGS sites. The sites are arranged according to the tectonic domain. One epoch of campaign measurement contains 3–6 days (24 h session) of GPS data, and each epoch is separated by minimum of 1 year. Permanent station data are continuous (24 × 7, 365 days a year) with few data gaps

and m denotes total slip associated with the rectangular fault (combination of dip slip and strike slip) responsible for the surface deformation. Weighted least-squares inversion of the above observation equation gives the slip m as

$$m = \left[G^T W_e G \right]^{-1} G^T W_e d \qquad (2)$$

here W_e is the weight matrix. The initial values of the dislocation parameters are obtained from earthquake focal mechanisms and fault mapping. The weight matrix is taken as the inverse of covariance matrix of the observed GPS displacements. The inversion computer program accepts a range of values for the initial dislocation parameters and GPS-derived surface displacements as input and computes slip by varying the dislocation parameters within the given input range. The best fit model is the one for which the residual between the observed and modelled displacements is minimal. Computations are performed iteratively yielding the final fault parameters that best match the GPS-observed surface deformation pattern.

Results

The estimated rates and standard deviation of displacement of the campaign as well as permanent GPS stations in ITRF2008 and India-fixed reference frame are given in Table 2. The India-fixed velocities are plotted in Fig. 2. We discuss the contemporary surface deformation rates in Shillong Plateau, Assam Valley, Eastern Himalaya and Indo-Burmese Fold and Thrust Belt of north-eastern India in subsequent sections.

Shillong Plateau

Shillong Plateau is an elevated block bounded in the south by Dauki fault and in the north by Assam Valley. Dudhnoi fault is located at the western Shillong Plateau, and Kopili fault is located to the northeast of the plateau in Assam Valley (Duarah and Phukan 2011; Baruah et al. 2011; Kayal et al. 2012). The sites situated on central Shillong Plateau show ~7.5 ± 0.3 mm/year southward velocities (Fig. 2) in Indian reference frame. We observe similar southward velocity of ~7 ± 0.3 mm/year of sites located in Assam Valley north of the plateau (e.g. GARO, BAMU, and GHTU). Since sites MAWR, NONG, CSOS, MUNN, GHTU, BAMU, and GARO move coherently, we assume that they lie on a nearly rigid block and estimate the Euler pole of rotation of Shillong Plateau–Assam Valley (SH–AS) relative to India to be located at −25.1° ± 0.2°N, −97.8° ± 1.8°E with angular velocity of 0.533° ± 0.10°/Myr. The clockwise rotation of the SH–AS thus is broadly consistent with the clockwise rotation of Shillong Plateau

Fig. 2 Estimated velocities of GPS sites in India-fixed reference frame. Velocity vectors are tipped with 95 % confidence error ellipse. Location of two GPS sites TURA and MOPEN (Jade et al. 2007) are marked in the figure. *MCT* Main Central Thrust, *MBT* Main Boundary Thrust, *C.F.* Chedrang Fault, *Du. F.* Dudhnoi fault, *B.S.Z.* Barapani Shear Zone, *SP* Shillong Plateau, *MH* Mikir Hills, *C.M.F.* Churachandpur-Mao Fault
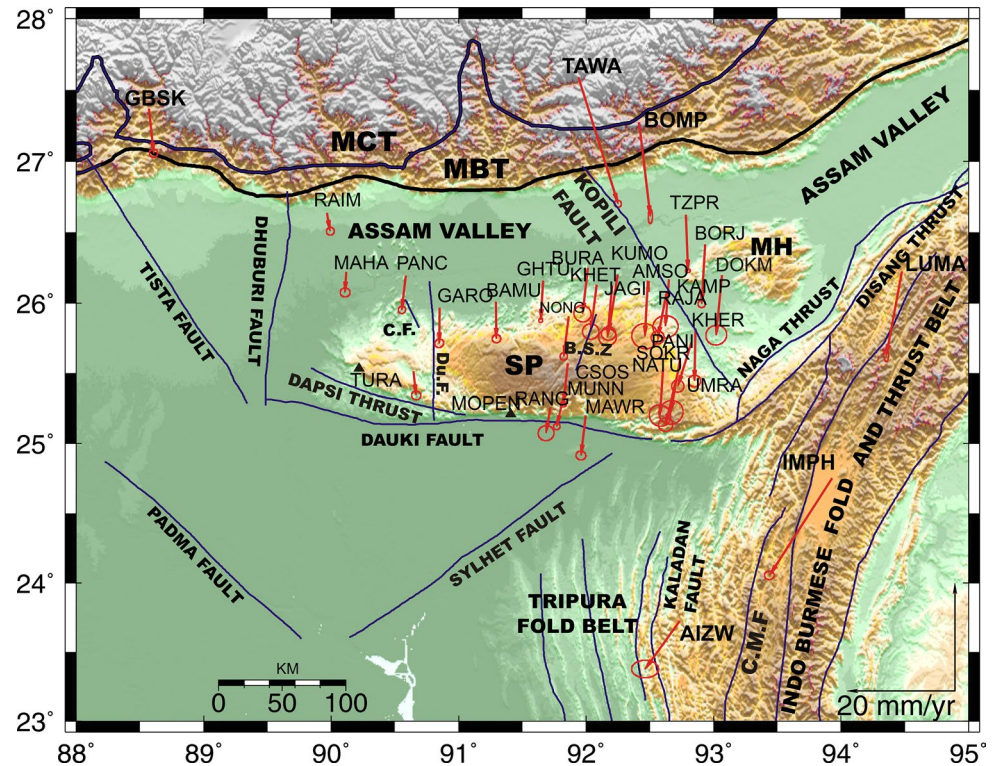
and Assam Valley reported by Vernant et al. 2014. Sites located in central Shillong Plateau and Assam Valley north of the plateau (Fig. 3) show statistically insignificant residuals in SH–AS-fixed reference frame. Most of the Shillong Plateau site velocities (except WLMN, RANG) are also statistically insignificant (Fig. 3) which is consistent with the rates reported by Jade et al. (2007), i.e. that the central Shillong Plateau behaves like a rigid block with ~7 mm/year southward velocity (Fig. 2) and no current local deformation is taking place.

The site WLMN located to the west of Dudhnoi fault on western Shillong Plateau (Fig. 3) shows SH–AS-fixed velocity of 2.4 ± 0.3 mm/year NE. This high velocity difference compared to central Shillong Plateau suggests different tectonic setting of western Shillong Plateau compared to central plateau. Earlier studies (Jade et al. 2007; Mukul et al. 2010) have reported high velocity (5.7 ± 1 mm/year) relative to CSOS, for a GPS site TURA located at the western margin of the plateau (Fig. 3). The western Shillong Plateau was the site for the 1897 great Shillong earthquake which caused an 11-m co-seismic slip down to the west of the Chedrang River and activated the Dudhnoi and Chedrang fault (Oldham 1899). The western Shillong Plateau crust is found thinner (~33 km) compared to the central Shillong Plateau (~35–38 km) (Bora and Baruah 2012). This thinner crust of western Shillong Plateau has broken down along Dudhnoi fault in 1897 great event. Recent aeromagnetic survey over Shillong Plateau

reports uplifted block in NW–SE direction within a broad depressed block north of Tura (Sharma et al. 2012). Also, Dapsi Thrust lies towards the western end of Shillong Plateau. These observations suggest tectonic setting of the western Shillong Plateau is not similar to that of the central Shillong Plateau which may have contributed to this relative velocity and needs further corroboration.

RANG GPS site with data spanning 10 years (2003–2013) located further west of MAWR indicates northward motion of 2.6 ± 0.6 mm/year. Earlier study by Mukul et al. (2010) reports 1.5–3.5 mm/year convergence in Shillong Plateau based on the baseline length change between Guwahati and a site Mopen (25.23°N, 91.44°E) (Fig. 3). Mopen is situated west of RANG at almost same latitude, and both shows velocities different from central Shillong Plateau. The Nohkalikai Falls which is the tallest waterfall in India is just 3.6 km away from the RANG site and the topography of the plateau drops by nearly 340 m near this fall. There is high possibility of ongoing local deformation towards the southern edge of Shillong Plateau and need further investigation.

To the east of Shillong Plateau, campaign site UMRA indicates SW velocity of 2.4 ± 0.5 mm/year, whereas SOKR and NATU sites record statistically insignificant residual velocities in SH–AS reference frame. Kopili River originates between UMRA and NATU and exhibits neotectonic activities like hot-water springs, deep gorges, many rapids, and falls. These sites are located towards the

Fig. 3 Velocities in Shillong Plateau–Assam Valley (SH–AS) reference frame (See text for details). Velocity vectors are tipped with 70 % confidence error ellipse. Location of two GPS sites TURA and MOPEN (Jade et al. 2007) are marked in the figure. *C.F.* Chedrang Fault, *Du. F.* Dudhnoi fault, *B.S.Z.* Barapani Shear Zone
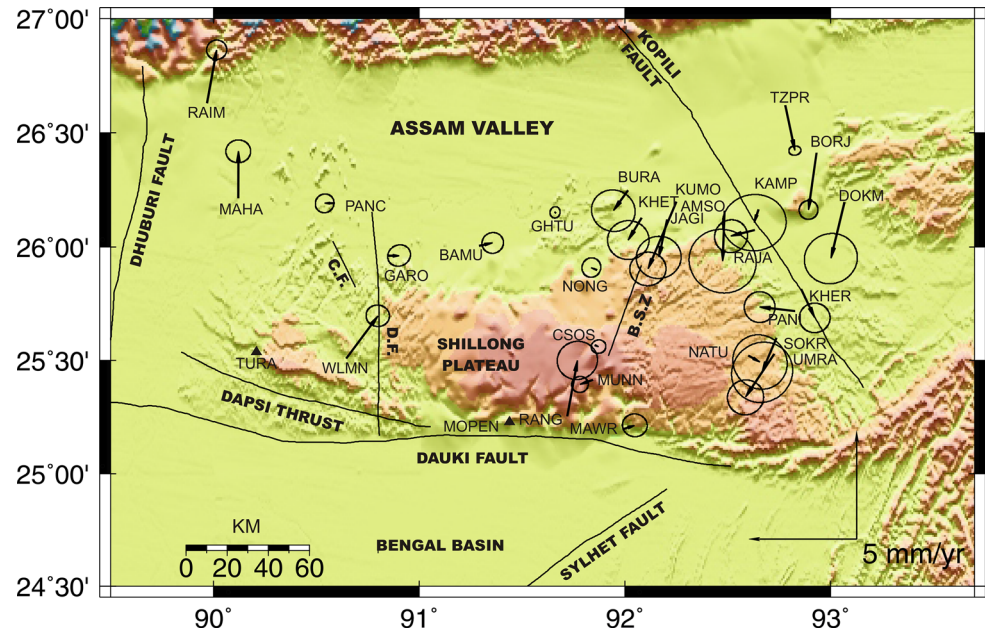
southern end of the Kopili fault where high stress concentration was reported by Bhattacharya et al. (2008). This region requires further study with dense GPS measurements as there is high probability that the Kopili fault may be passing through this foreland of the plateau.

Assam Valley

India-fixed velocities of Assam Valley GPS sites (Fig. 2) vary significantly (3–11 mm/year SSW) from RAIM in the west to TZPR to the east. The strong velocity gradient between MAHA (~3 mm/year S) and the GPS sites (PANC, GARO, BAMU) to the east with ~6.5 mm/year southward velocity indicates that the two known faults viz. Chedrang and Dudhnoi fault (Fig. 1) in this region may be active. The Assam Valley GPS sites just east of Guwahati (BURA, KHET, JAGI, AMSO, and KUMO) have velocities ~8–11 mm/year SW in Indian reference frame, with more southward motion (west component being nearly same). Further to the east, the two sites BORJ (10.9 ± 0.3 mm/year) and DOKM (11.5 ± 0.8 mm/year) situated at the western margin of Mikir Hills have further increase in south-westward motion in Indian reference frame. These velocities imply deformation is not uniform across the Assam Valley, and it increases from west to east with a superimposed clockwise rotation.

Velocities of the Assam Valley GPS sites situated outside the SH–AS reference frame (Fig. 3) indicate clockwise rotation of the north-eastern segment of the Indian plate with differential motion across the Kopili fault consistent with that reported by Vernant et al. (2014). The far sites MAHA and RAIM situated on the western margin

of Assam Valley show ~2.3 mm/year of north-directed motion, whereas the eastern sites record ~2–3 mm/year SSW motion. The northward motion (~2.3 mm/year) of western Assam Valley sites includes a component of N–S India-Eurasia plate convergence, whereas the 2–3 mm/year oblique motion of eastern Assam Valley sites includes a component of Kopili fault motion, clockwise rotation of SH–AS block as well as N–S convergence due to India-Eurasia collision.

Kopili fault

Kopili fault is an active fault running obliquely in NW–SE direction separating the Shillong Plateau and Mikir massif as well as the Assam Valley. Fault parallel component of SH–AS-fixed velocities of all the sites located in the vicinity of Kopili fault is plotted in Fig. 4. Arc-tangent profile fit (Savage and Burford 1970) to fault parallel velocities (Fig. 4) of the GPS sites (BORJ, DOKM, TZPR, KAMP, RAJA, PANI) estimates dextral shear of 4.7 ± 1.3 mm/year and a locking depth of 10.2 ± 1.4 km for Kopili fault. KHER GPS site situated at less than 1 km from the fault trace is treated as an outlier. The fault parallel velocities of GPS sites located to the west of Kopili fault at the northeastern and eastern margin of Shillong Plateau (BURA, KHET, JAGI, AMSO, KUMO, SOKR, UMRA) indicate a composite effect of N–S Indo-Eurasian convergence, dextral shear of Kopili fault and clockwise rotation of SH–AS block. Low-magnitude (<5 Mw) earthquakes are frequent in the Kopili fault region. A 5.4 Mw event occurred on 11 May 2012 (USGS earthquake catalogue). These events lower the strain accumulation of the fault. The dextral shear
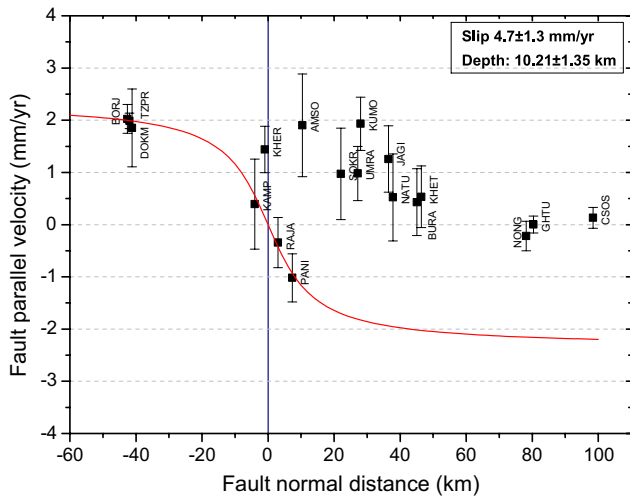
Fig. 4 Kopili fault parallel velocities in SH–AS reference frame showing the dextral shear of the fault. The *red line* is the best fit arctangent profile using six GPS sites TZPR, DOKM, BORJ, KAMP, PANI, and RAJA

of Kopili fault (Fig. 4) affirms that Assam Valley is fragmented along fault and is consistent with the earlier studies (Mahesh et al. 2012; Vernant et al. 2014).

Eastern Himalaya

In order to quantify the deformation prevailing in Eastern Himalaya, we have used observations from the IGS site LHAZ situated on southern Tibet, TAWA situated immediate south of the Tibetan Plateau, BOMP on foot-wall of MCT, GBSK in Sikkim Himalaya, RAIM located south of Bhutan Himalaya, and GHTU and TZPR on the foreland of the Himalayan convergence zone based on the widely accepted tectonic map of this region (Fig. 5). Arc-normal and arc-parallel velocity components at each of these sites are computed and plotted in Fig. 6. Results indicate total arc-normal convergence of around 16 mm/year in Sikkim and Arunachal Himalaya which is consistent with the earlier reported values in this region (Jade et al. 2007; Mukul et al. 2010). There is insignificant convergence between the campaign site TAWA and LHAZ (1.4 ± 0.3 mm/year), whereas we find 6.5 ± 0.8 mm/year convergence between TAWA and BOMP which represents the ongoing strain accumulation in higher Himalaya in MCT. Remaining ~10 mm/year arc-normal convergence is being accommodated in lesser Himalaya south of MCT indicating high strain accumulation. Eastern Himalaya exhibits relatively sparse seismic activity compared to the other sections of the Himalayan arc with two large earthquakes in this zone; one on 21 January 1941 (M 7.0) and the other on 29 July

1947 (M 7.8). Recently, spatio-temporal clustering of earthquakes near BOMP (82 events with Mb ≥ 4.5 spanning 1964–2006) has been identified (Mukhopadhyay et al. 2010) which also indicates high stress build-up and is being intermittently released by these minor events.

RAIM campaign site located on Indian plate just south of Bhutan MFT gives an arc-normal convergence rate of 19.2 ± 0.5 mm/year. This rate is ~3 mm/year higher than the earlier reported convergence rate of 16.5 ± 1.5 mm/year (Vernant et al. 2014) across western Bhutan Himalayas based on GPS sites situated just north of MFT. This rate is consistent with the geologic shortening rate of 20.8 ± 8.8 mm/year estimated for this section of the Himalayan arc (Berthet et al. 2014). Arc-parallel velocities indicate that there is no significant E–W deformation between Sikkim and Arunachal Himalaya which is consistent with the recent reported rates (Jade et al. 2014). The arc-parallel extension rate of ~5 mm/year between LHAZ, located in south Tibet and Sikkim-Arunachal Himalayan sites GBSK and BOMP (GBSK, 4.6 ± 0.5 mm/year and BOMP 5.5 ± 0.3 mm/year), represents a component of contemporary E–W extension rate in Tibet. This extension rate is consistent with the rates reported by other studies (Molnar and Tapponnier 1978; Larson et al. 1999; Chen et al. 2004; Jade et al. 2004; Zhang et al. 2004; Gan et al. 2007; Liang et al. 2013; Liu et al. 2014).

Single dislocation model of Jade et al. (2014) for Eastern Himalaya along the MHT (width 130 km, Depth 17 km and dip angle of 10°) is used to obtain the modelled velocities in northeast India. The observed and modelled velocities are plotted (Fig. 7) along the arc-normal profile (N83.96°E) with GHTU as origin. Dislocation models in Sikkim and Arunachal Himalaya give a slip rate of ~16–18 mm/year along MHT (Jade et al. 2014). The models also suggest that in this region, MHT is locked over a width of 105–130 km from the surface to a depth of 17–20 km with the underthrusting Indian plate. Recently, fault slip rates of 16.5–11.5 mm/year with variable width and locking depth were estimated (Vernant et al. 2014) in several segments of the Eastern Himalaya using DEFNODE (McCaffrey 2002). Our arc-normal convergence rates in Sikkim-Arunachal Himalaya are consistent with these models. Recent records of seismic activity (Mukhopadhyay et al. 2010) indicate that there is gradual stress build-up which may be released on reaching failure strain level thus putting this region under high seismic risk. This first-order simple dislocation model gives an estimate of the dislocation parameters of the Eastern Himalayan convergence and gives a reasonable fit to the GPS velocities. Separate dislocation models for Eastern Himalaya, Shillong–Assam block, and Kopili gap are required to better explain the observed velocities.
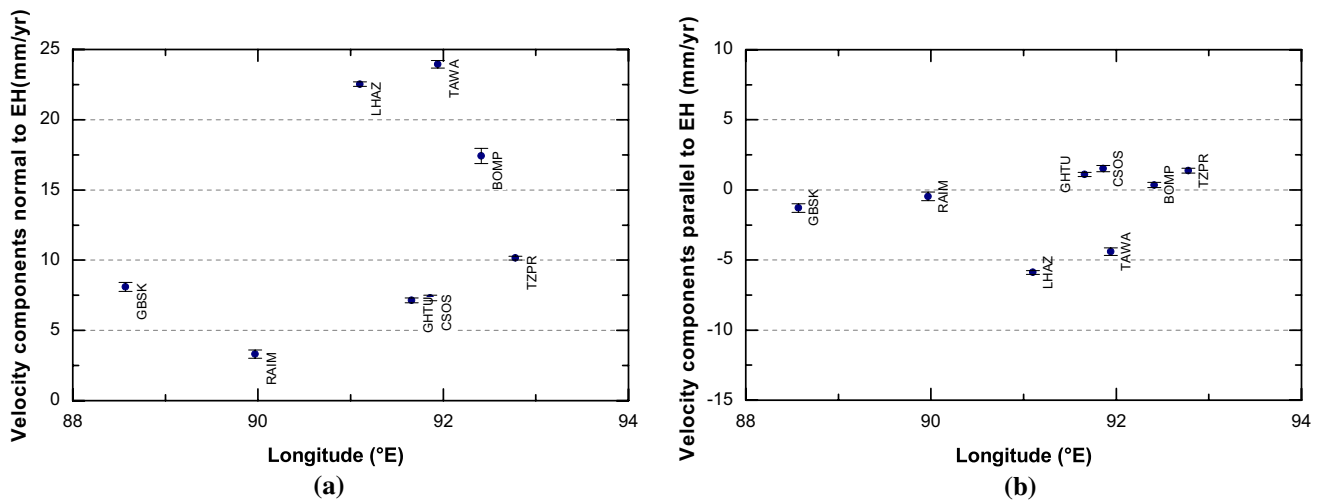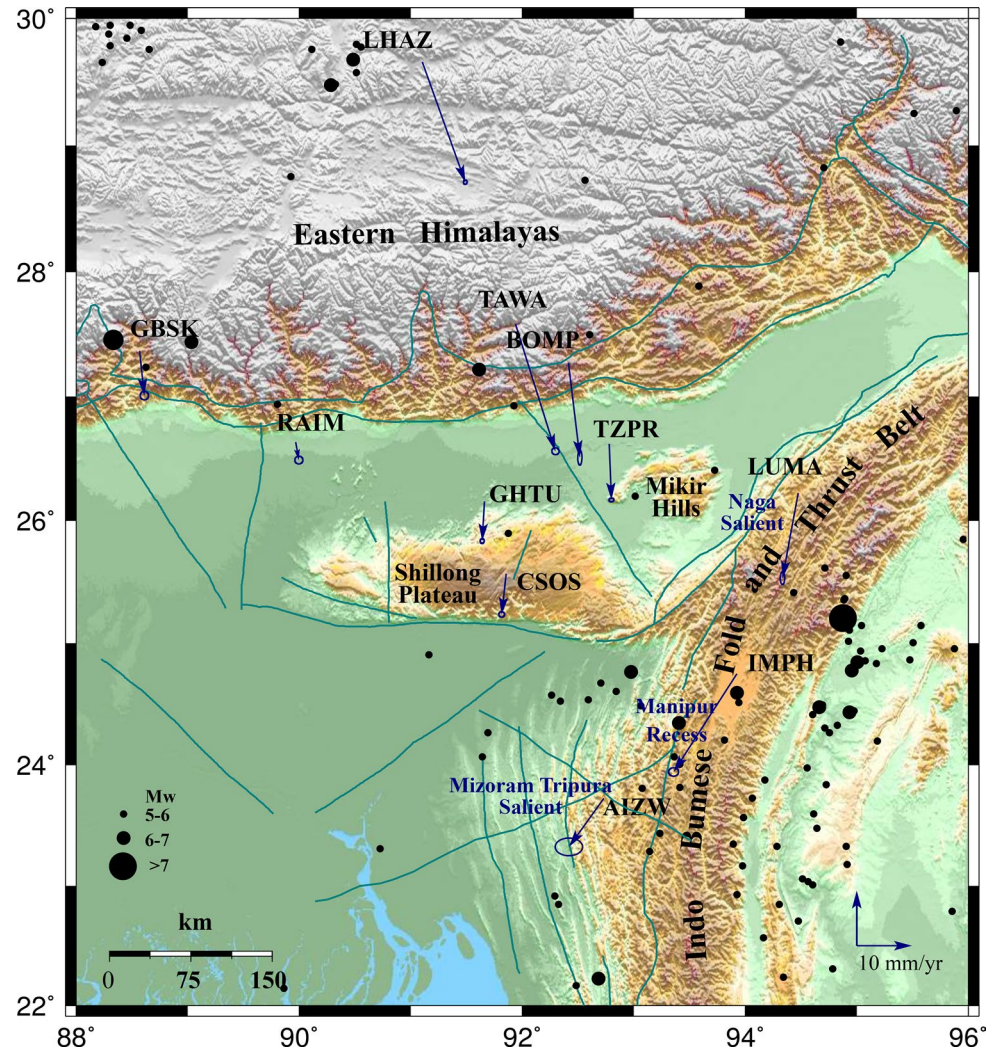
Fig. 6 India-fixed GPS velocities of Eastern Himalayan sites, resolved **a** normal and **b** parallel to the Eastern Himalayan (EH) arc

Fig. 7 India-fixed GPS velocities of sites situated at Arunachal Himalaya, Shillong Plateau and Assam Valley along arc-normal profile (N83.96°E) with Guwahati (GHTU) GPS site at the origin. Modelled velocities obtained using single dislocation for MHT (width 130 km, depth 17 km, and dip angle 10°) are shown in *black*. The best-fitting curve for both observed and modelled arc-normal velocities is shown in *red*
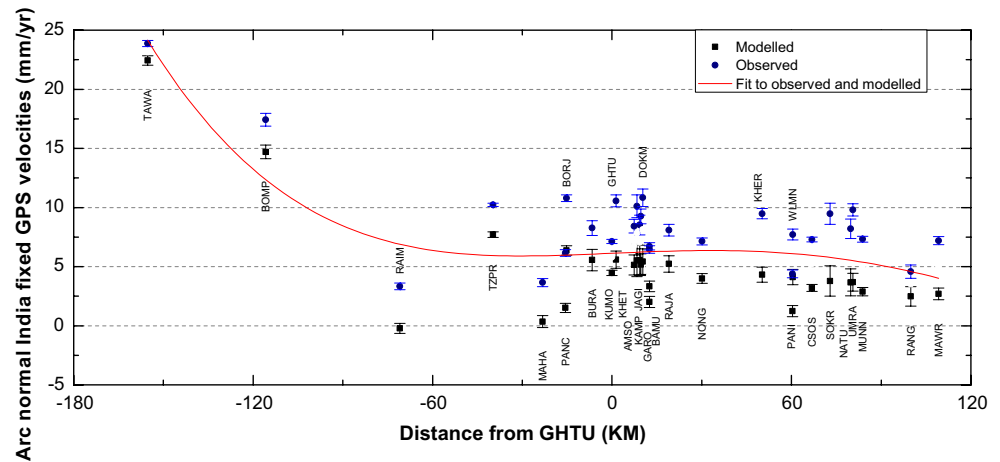
Indo-Burmese Fold and Thrust Belt

The Indo-Burmese Fold and Thrust Belt (IBFTB) is a complex geo-dynamical region where Indian plate is subducting below Sunda plate (Guzmán-Speziale and Ni 1996; Gahalaut et al. 2013). Many GPS-based studies report about 36 mm/year current convergence rate between Indian and Sunda plate (Vigny 2003; Socquet et al. 2006; Maurin et al. 2010; Gahalaut et al. 2013). IBFTB exhibit salient-recess topography, with parallel ridges and Valleys in curvilinear fashion which is typical feature of a fold and thrust belt resulting from subduction of the Indian plate beneath Sunda plate. Prominent thrusts that run parallel to the IBFTB are Kaladan fault, Churachandpur–Mao Fault, and Kabaw Fault from west to east (Fig. 1). The IBFTB is segmented by conjugate oblique/transverse faults. Many of the NW–SE oblique faults viz., Mat, Tuipui, Saitual, and Sateek faults in Mizoram are sinistral, whereas NE–SW oblique faults such as Amarpur, Gumti, Aizwal, and Kaladan lineament situated in Tripura Fold Belt are dextral in nature (Nandy 2001). There is ambiguity regarding the Kaladan fault, as initially the lineament located southeast of Lungleh, Mizoram, that followed the course of the Kaladan River in this region was named as Kaladan fault (Nandy 2001). The Kaladan fault referred by subsequent researchers as well in this text (Sikder and Alam 2003; Maurin and Rangin 2009; Gahalaut et al. 2013) is actually the contact between the Surma and Brail range and is named after the Kaladan River, as in Burma, the fault contact lies along the course of the said river (personal communication with Sujit Dasgupta, retired Deputy Director General, GSI, India).

We have continuous GPS data from three permanent sites LUMA, IMPH, and AIZW, situated along the western edge of the IBFTB. LUMA is situated at Naga Salient; IMPH at Manipur recess and AIZW at Tripura-Mizoram

Salient (Fig. 5). GPS velocities of these three IBFTB sites along with the permanent sites located in Shillong Plateau and Assam Valley (CSOS, GHTU and TZPR) are resolved normal and parallel to IBFTB to study the deformation pattern in this region (Fig. 8). Published studies report about 36 mm/year relative plate motion between India and Sunda plates, of which around 16 mm/year motion is occurring in the IBFTB and the remaining 20 mm/year is occurring in the Sagaing fault by dextral motion (Vigny 2003; Socquet et al. 2006; Maurin et al. 2010). The 16 mm/year motion in western IBFTB is occurring without any strain accumulation (i.e. aseismic slip) between east of Churachandpur–Mao fault and to the west of the Sagaing fault (Gahalaut et al. 2013). The GPS site velocities of the present study indicate that the 16 mm/year motion in western segment of IBFTB has a normal component of ~6 ± 0.7 mm/year between LUMA-IMPH and variable parallel component 6.9 ± 0.7 mm/year between LUMA-IMPH and 10.5 ± 1.1 mm/year between IMPH-AIZW (Fig. 8). India-fixed GPS velocities of IBFTB sites (Fig. 2) indicate oblique motion of ~15.7 ± 0.5 mm/year at LUMA and IBFTB parallel motion of ~21.3 ± 0.4 and 10.9 ± 0.8 mm/year at Imphal and Aizwal, respectively. The baseline length LUMA-IMPH indicates an extension of 4.8 ± 0.5 mm/year, whereas IMPH-AIZW indicates a shortening of 10.1 ± 0.9 mm/year. These rates affirms that the deformation in IBFTB is segmented into N–S blocks along E–W transverse zones exhibiting oblique motion between Naga Salient–Manipur Recess and arc-parallel motion between Manipur Recess–Tripura-Mizoram Salient. Velocities of Shillong Plateau and Assam Valley continuous GPS sites north to the plateau indicate normal convergence of ~3 mm/year (Fig. 8a) with IBFTB related to India-Sunda plate subduction. This rate is broadly consistent with the rate of convergence of Shillong Plateau and IBFTB given by Mukul et al. (2010).
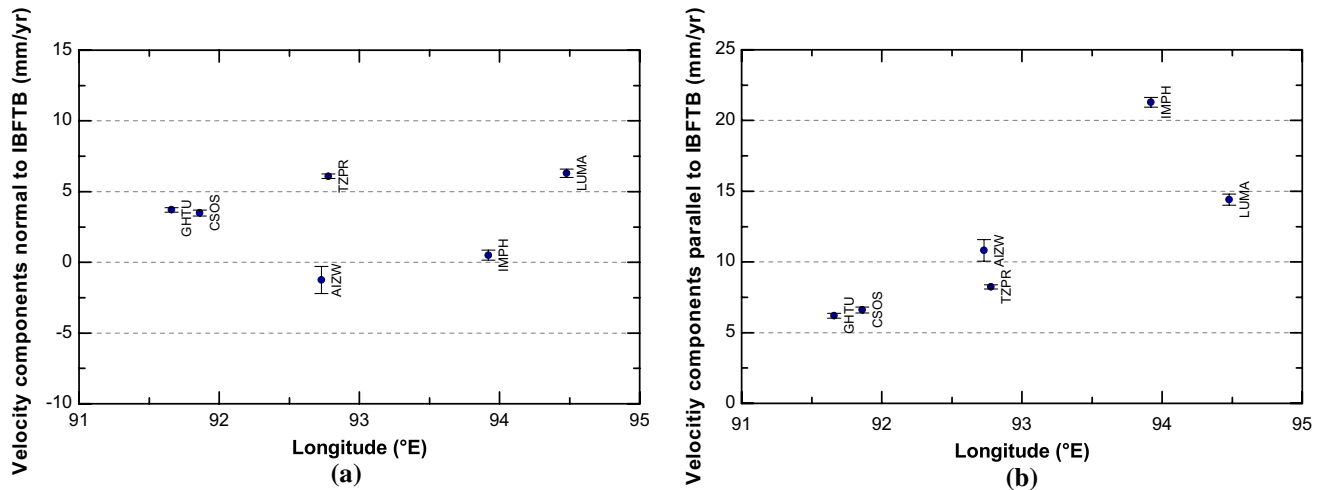
Fig. 8 India-fixed GPS velocities of sites related to Indo-Burmese region resolved **a** normal and **b** parallel to IBFTB

Discussion

In this study, crustal displacement rates are estimated for the first time using 11 years of GPS observations. These rates suggest high stress accumulation and strain build-up in the different tectonic domains of northeast India indicating high seismic vulnerability of this region which poses great threat to the large population of the northeast Indian states and neighbouring Bangladesh. This region warrants further detailed studies with dense network of GPS measurements in Shillong Plateau, Assam Valley, Kopili fault, Eastern Himalaya, and Indo-Burmese region. Significant insights of the dynamics of this tectonically complex region from the present study are given below.

The central Shillong Plateau and Assam Valley north of Plateau (SH–AS) behave like a rigid block with ~7 mm/year southward velocity in India-fixed reference frame. Euler pole of rotation of SH–AS block in Indian reference frame estimated using GPS sites having coherent velocities in central Shillong Plateau and Assam Valley north of plateau indicate clockwise rotation of the block. SH–AS-fixed velocities indicate insignificant residuals in central Shillong Plateau and Assam Valley north of the Plateau. Assam Valley GPS sites indicate gradual increase (~3–11 mm/year) in India-fixed velocities from west to east and SH–AS-fixed velocities indicate clockwise rotation of Assam Valley sites outside the SH–AS reference frame. Rotational component of Shillong Plateau and Assam Valley is due to the unique tectonic setting of this region which is under influence of both the Indo-Eurasia convergence in Eastern Himalaya and Assam syntaxis as well as oblique convergence between India-Sunda plates along IBFTB. GPS observations indicate 4.7 ± 1.3 mm/year of dextral motion along Kopili fault with a locking depth of 10.2 ± 1.4 km.

Results suggest that Assam Valley is fragmented across the Kopili fault with the eastern fragment moving southwards at higher rate than the western fragment. Results indicate that west side of Mikir Massif moves as a rigid block and is presently locked to Assam Valley.

For the first time, arc-normal convergence rate of ~19 mm/year is obtained in Bhutan Himalaya using GPS observations. Arc-normal convergence rate of ~16 mm/year in Sikkim and Arunachal Himalaya obtained from the present study is consistent with the earlier reported rates (Jade et al. 2007; Mukul et al. 2010). Present-day arc-normal convergence of ~16 mm/year in Arunachal Himalayas is distributed between the Higher (~6 mm/year) and the Lesser (~10 mm/year) Himalayas indicating high strain accumulation in this region. First-order dislocation model of this region gives a reasonable fit to the observed velocities, suggesting that MHT is locked from the surface to a depth of 17 km and has a slip rate of ~16 mm/year which is similar to that reported by Jade et al. (2014) and Vernant et al. (2014).

There is no significant arc-parallel (E–W) deformation in Sikkim-Arunachal Himalaya. Arc-Parallel extension rate of ~5 mm/year between LHAZ in south Tibet and Eastern Himalaya represents the component of the eastward extrusion of Tibet Plateau which also includes deformation resulting from the curvature of locked MHT. The arc-parallel velocities are consistent with the hypothesis of eastward extrusion of the Tibetan Plateau around the Assam syntaxis as reported by earlier researchers (Molnar and Tapponnier 1978; Larson et al. 1999; Chen et al. 2004; Jade et al. 2004; Zhang et al. 2004; Gan et al. 2007; Liang et al. 2013; Liu et al. 2014).

Indo-Burmese Fold and Thrust Belt is accommodating ~16 mm/year of the India-Sunda relative plate motion of

36 mm/year and the rest being accommodated at the Sagaing fault. This 16 mm/year motion in IBFTB consists of normal compression of ~6 mm/year between LUMA-IMPH as well as IBFTB parallel slip of ~7–11 mm/year between LUMA-IMPH and IMPH-AIZW, respectively. Oblique velocity at LUMA and arc-parallel velocity at IMPH and AIZW (Fig. 5) indicate that the deformation in IBFTB varies from Naga Salient in the north to Tripura-Mizoram Salient in the south and there is relative motion between the Salients and Recesses. Deformation rates in IBFTB indicate high seismic vulnerability of this region. IBFTB is segmented with several oblique/transverse faults (Nandy 2001) trending NE–SW (dextral in nature) and NW–SE (sinistral in nature) and quantification of the variation of deformation along these faults is crucial. Recently, it has been debated whether the 2004 Andaman–Sumatra mega event raised the risk of future tsunamigenic earthquakes in northern Bay of Bengal (Ioualalen et al. 2007; Cummins 2007; Gupta and Gahalaut 2009). The focal mechanism solution of the earthquakes occurring along the Indo-Burmese accretionary wedge (Fig. 1) indicates strike-slip faulting and north–south shortening parallel to the eastern margin of the Indian plate (Ni et al. 1989). This oblique convergence of India-Sunda plate along the Indo-Burmese Fold and Thrust Belt, absorbed by the strike-slip movement as shown by our study, indicates reduced potential for future tsunamigenic earthquakes in the Northern Bengal Basin. Further, should an earthquake occur in this region, the thick sediments of the Bengal fan will contribute towards reduction in the amplitude of the seismic waves as demonstrated by numerical modelling (Ioualalen et al. 2007).

Compliance with ethical standards

Conflict of interest The authors declare no conflict of interest.

References

Altamimi Z, Collilieux X, Métivier L (2011) ITRF2008: an improved solution of the international terrestrial reference frame. J Geod 85:457–473. doi:10.1007/s00190-011-0444-4

Baruah S, Baruah S, Kalita A, Kayal JR (2011) Ground motion parameters in Shillong and Mikir Plateau supplemented by mapping of amplification factors in Guwahati City, Northeastern India. J Asian Earth Sci 42:1424–1436. doi:10.1016/j.jseaes.2011.06.006

Ben-Menahem A, Aboodi E, Schild R (1974) The source of the great Assam earthquake—an interplate wedge motion. Phys Earth Planet Inter 9:265–289. doi:10.1016/0031-9201(74)90056-9

Berthet T, Ritz J-F, Ferry M et al (2014) Active tectonics of the eastern Himalaya: new constraints from the first tectonic geomorphology study in southern Bhutan. Geology 42:427–430. doi:10.1130/G35162.1

Bhattacharya PM, Mukhopadhyay S, Majumdar RK, Kayal JR (2008) 3-D seismic structure of the northeast India region and its implications for local and regional tectonics. J Asian Earth Sci 33:25–41. doi:10.1016/j.jseaes.2007.10.020

Bilham R, England P (2001) Plateau "pop-up" in the great 1897 Assam earthquake. Nature 410:806–809. doi:10.1038/35071057

Bilham R, Larson KM, Freymueller JT (1997) GPS measurements of present-day convergence across the Nepal Himalaya. Nature 386:61–64. doi:10.1038/386061a0

Bora DK, Baruah S (2012) Mapping the crustal thickness in Shillong–Mikir Hills Plateau and its adjoining region of northeastern India using Moho reflected waves. J Asian Earth Sci 48:83–92. doi:10.1016/j.jseaes.2011.12.007

Chen W-P, Molnar P (1977) Seismic moments of major earthquakes and the average rate of slip in central Asia. J Geophys Res 82:2945–2969. doi:10.1029/JB082i020p02945

Chen W-P, Molnar P (1990) Source parameters of earthquakes and intraplate deformation beneath the Shillong Plateau and the Northern Indoburman ranges. J Geophys Res 95:12527. doi:10.1029/JB095iB08p12527

Chen Q, Freymueller JT, Wang Q et al (2004) A deforming block model for the present-day tectonics of Tibet. J Geophys Res 109:B01403. doi:10.1029/2002JB002151

Clark M, Bilham R (2008) Miocene rise of the Shillong Plateau and the beginning of the end for the Eastern Himalaya. Earth Planet Sci Lett 269:337–351. doi:10.1016/j.epsl.2008.01.045

Copley A, McKenzie D (2007) Models of crustal flow in the India–Asia collision zone. Geophys J Int 169:683–698. doi:10.1111/j.1365-246X.2007.03343.x

Cummins PR (2007) The potential for giant tsunamigenic earthquakes in the northern Bay of Bengal. Nature 449:75–78. doi:10.1038/nature06088

Devachandra M, Kundu B, Catherine J et al (2014) Global positioning system (GPS) measurements of crustal deformation across the frontal Eastern Himalayan syntaxis and seismic-hazard assessment. Bull Seismol Soc Am. doi:10.1785/0120130290

Dong D, Herring TA, King RW (1998) Estimating regional deformation from a combination of space and terrestrial geodetic data. J Geod 72:200–214

Duarah BP, Phukan S (2011) Understanding the tectonic behaviour of the Shillong plateau, India using remote sensing data. J Geol Soc India 77:105–112

Estey LH, Meertens CM (1999) TEQC: the multi-purpose toolkit for GPS/GLONASS data. GPS Solut 3:42–49. doi:10.1007/PL00012778

Gahalaut VK, Kundu B, Laishram SS et al (2013) Aseismic plate boundary in the Indo-Burmese wedge, northwest Sunda Arc. Geology 41:235–238. doi:10.1130/G33771.1

Gan W, Zhang P, Shen Z-K et al (2007) Present-day crustal motion within the Tibetan Plateau inferred from GPS measurements. J Geophys Res 112:B08416. doi:10.1029/2005JB004120

Gupta H, Gahalaut VK (2009) Is the Northern Bay of Bengal Tsunamigenic? Bull Seismol Soc Am 99:3496–3501. doi:10.1785/0120080379

Guzmán-Speziale M, Ni JF (1996) Seismicity and active tectonics of the western Sunda Arc. In: Yin A, Harrison TM (eds) The Tectonic Evolution of Asia. Cambridge University Press, Cambridge, pp 63–84

Herring TA (2003) MATLAB tools for viewing GPS velocities and time series. GPS Solut 7:194–199. doi:10.1007/s10291-003-0068-0

Herring TA, King RW, Mcclusky SC (2010a) Documentation of the GAMIT GPS analysis software release 10.4. Department of Earth, and Planetary Sciences, Massachusetts Institute of Technology, Cambridge

Herring TA, King RW, Mcclusky SC (2010b) GLOBK, Global Kalman filter VLBI and GPS analysis program version 10.4. Department of Earth, and Planetary Sciences, Massachusetts Institute of Technology, Cambridge

Ioualalen M, Pelinovsky E, Asavanant J et al (2007) On the weak impact of the 26 December Indian Ocean tsunami on the Bangladesh coast. Nat Hazards Earth Syst Sci 7:141–147. doi:10.5194/nhess-7-141-2007

Jade S, Bhatt BC, Yang Z et al (2004) GPS measurements from the Ladakh Himalaya, India: preliminary tests of plate-like or continuous deformation in Tibet. Geol Soc Am Bull 116:1385. doi:10.1130/B25357.1

Jade S, Mukul M, Bhattacharyya AK et al (2007) Estimates of interseismic deformation in Northeast India from GPS measurements. Earth Planet Sci Lett 263:221–234. doi:10.1016/j.epsl.2007.08.031

Jade S, Mukul M, Gaur VK et al (2014) Contemporary deformation in the Kashmir-Himachal, Garhwal and Kumaon Himalaya: significant insights from 1995–2008 GPS time series. J Geod. doi:10.1007/s00190-014-0702-3

Kayal JR, De R (1991) Microseismicity and tectonics in Northeast India. Bull Seismol Soc Am 81:131–138

Kayal JR, Arefiev SS, Baruah S et al (2012) Large and great earthquakes in the Shillong plateau–Assam valley area of Northeast India region: pop-up and transverse tectonics. Tectonophysics 532–535:186–192. doi:10.1016/j.tecto.2012.02.007

Larson KM, Bürgmann R, Bilham R, Freymueller JT (1999) Kinematics of the India-Eurasia collision zone from GPS measurements. J Geophys Res 104:1077–1093. doi:10.1029/1998JB900043

Liang S, Gan W, Shen C et al (2013) Three-dimensional velocity field of present-day crustal motion of the Tibetan Plateau derived from GPS measurements. J Geophys Res Solid Earth 118:5722–5732. doi:10.1002/2013JB010503

Liu QY, van der Hilst RD, Li Y et al (2014) Eastward expansion of the Tibetan Plateau by crustal flow and strain partitioning across faults. Nat Geosci 7:361–365. doi:10.1038/ngeo2130

Mahesh P, Catherine JK, Gahalaut VK et al (2012) Rigid Indian plate: constraints from GPS measurements. Gondwana Res 22:1068–1072. doi:10.1016/j.gr.2012.01.011

Maurin T, Rangin C (2009) Structure and kinematics of the Indo-Burmese Wedge: recent and fast growth of the outer wedge. Tectonics. doi:10.1029/2008TC002276

Maurin T, Masson F, Rangin C et al (2010) First global positioning system results in northern Myanmar: constant and localized slip rate along the Sagaing fault. Geology 38:591–594. doi:10.1130/G30872.1

McCaffrey R (2002) Crustal block rotations and plate coupling. In: Stein S, Freymueller JT (eds) Plate boundary zones. American Geophysical Union, Washington, D.C., pp 101–122

Molnar P, Tapponnier P (1978) Active tectonics of Tibet. J Geophys Res 83:5361. doi:10.1029/JB083iB11p05361

Mukhopadhyay B, Acharyya A, Dasgupta S (2010) Potential source zones for Himalayan earthquakes: constraints from spatial–temporal clusters. Nat Hazards 57:369–383. doi:10.1007/s11069-010-9618-2

Mukul M, Jade S, Bhattacharyya AK, Bhusan K (2010) Crustal shortening in convergent orogens: insights from global positioning system (GPS) measurements in Northeast India. J Geol Soc India 75:302–312

Nandy DR (2001) Geodynamics of Northeastern India and the adjoining region. ACB Publications, Kolkata

Ni JF, Guzmán-Speziale M, Bevis M et al (1989) Accretionary tectonics of Burma and the three-dimensional geometry of the Burma subduction zone. Geology 17:68–71

Okada Y (1985) Surface deformation due to shear and tensile faults in a half-space. Bull Seismol Soc Am 75:1135–1154

Oldham RD (1899) Report on the Great Earthquake of 12th June 1897. Office of the Geological survey

Paul J, Bürgmann R, Gaur VK et al (2001) The motion and active deformation of India. Geophys Res Lett 28:647. doi:10.1029/2000GL011832

Petrie EJ, King MA, Moore P, Lavallée DA (2010) Higher-order ionospheric effects on the GPS reference frame and velocities. J Geophys Res 115:B03417. doi:10.1029/2009JB006677

Reilinger R, McClusky S, Vernant P et al (2006) GPS constraints on continental deformation in the Africa-Arabia-Eurasia continental collision zone and implications for the dynamics of plate interactions. J Geophys Res 111:B05411. doi:10.1029/2005JB004051

Savage JC, Burford RO (1970) Accumulation of tectonic strain in California. Bull Seismol Soc Am 60:1877–1896

Schaer S, Gurtner W, Feltens J (1998) IONEX: the ionosphere map exchange format version 1. In: Proceedings of the IGS AC workshop, vol 9. Darmstadt, Germany

Sharma R, Gouda HC, Singh RK, Nagaraju BV (2012) Structural study of Meghalaya Plateau through aeromagnetic data. J Geol Soc India 79:11–29

Sikder AM, Alam MM (2003) 2-D modelling of the anticlinal structures and structural development of the eastern fold belt of the Bengal Basin, Bangladesh. Sediment Geol 155:209–226. doi:10.1016/S0037-0738(02)00181-1

Socquet A, Vigny C, Chamot-rooke N et al (2006) India and Sunda plates motion and deformation along their boundary in Myanmar determined by GPS. J Geophys Res 111:B05406. doi:10.1029/2005JB003877

Vasilief I (2011) QtiPlot: data analysis and scientific visualization. http://www.qtiplot.com/index.html.

Vernant P, Bilham R, Szeliga W et al (2014) Clockwise rotation of the Brahmaputra valley relative to India: tectonic convergence in the eastern Himalaya, Naga Hills, and Shillong Plateau. J Geophys Res Solid Earth 119:6558–6571. doi:10.1002/2014JB011196

Vigny C (2003) Present-day crustal deformation around Sagaing fault, Myanmar. J Geophys Res 108:2533. doi:10.1029/2002JB001999

Wessel P, Smith WHF, Scharroo R et al (2013) Generic mapping tools: improved version released. EOS Trans Am Geophys Union 94:409–410. doi:10.1002/2013EO450001

Zhang P-Z, Shen Z, Wang M et al (2004) Continuous deformation of the Tibetan Plateau from global positioning system data. Geology 32:809. doi:10.1130/G20554.1